

OPEN

Neurology®

The most widely read and highly cited peer-reviewed neurology journal
The Official Journal of the American Academy of Neurology



Neurology Publish Ahead of Print
DOI: 10.1212/WNL.0000000000200573

Neuropathologic Features of Antemortem Atrophy-Based Subtypes of Alzheimer Disease

Author(s):

Rosaleena Mohanty, PhD¹; Daniel Ferreira, PhD^{1,2}; Simon Frerich, MSc^{1,3}; J-Sebastian Muehlboeck, MSc¹; Michel J. Grothe, PhD^{4,5}; Eric Westman, PhD^{1,6} on behalf of For the Alzheimer's Disease Neuroimaging Initiative

This is an open access article distributed under the terms of the Creative Commons Attribution License 4.0 (CC BY), which permits unrestricted use, distribution, and reproduction in any medium, provided the original work is properly cited.

Neurology® Published Ahead of Print articles have been peer reviewed and accepted for publication. This manuscript will be published in its final form after copyediting, page composition, and review of proofs.

Errors that could affect the content may be corrected during these processes.

Corresponding Author:

Rosaleena Mohanty, rosaleena.mohanty@ki.se

Affiliation Information for All Authors: 1. Division of Clinical Geriatrics, Department of Neurobiology, Care Sciences and Society, Karolinska Institutet, Stockholm, Sweden; 2. Department of Radiology, Mayo Clinic, Rochester, MN, United States; 3. Institute for Stroke and Dementia Research, University Hospital, Ludwig-Maximilians-University (LMU) Munich, Munich, Germany; 4. Unidad de Trastornos del Movimiento, Servicio de Neurología y Neurofisiología Clínica, Instituto de Biomedicina de Sevilla, Hospital Universitario Virgen del Rocío/CSIC/Universidad de Sevilla, Seville, Spain; 5. Clinical Dementia Research Section, German Center for Neurodegenerative Diseases (DZNE), Rostock, Germany; 6. Department of Neuroimaging, Centre for Neuroimaging Sciences, Institute of Psychiatry, Psychology and Neuroscience, King's College London, London, UK

Neurology® Published Ahead of Print articles have been peer reviewed and accepted for publication. This manuscript will be published in its final form after copyediting, page composition, and review of proofs. Errors that could affect the content may be corrected during these processes.

Equal Author Contribution:**Contributions:**

Rosaleena Mohanty: Drafting/revision of the manuscript for content, including medical writing for content; Study concept or design; Analysis or interpretation of data

Daniel Ferreira: Drafting/revision of the manuscript for content, including medical writing for content; Study concept or design

Simon Frerich: Analysis or interpretation of data

J-Sebastian Muehlboeck: Analysis or interpretation of data

Michel J. Grothe: Drafting/revision of the manuscript for content, including medical writing for content; Study concept or design

Eric Westman: Drafting/revision of the manuscript for content, including medical writing for content; Study concept or design; Analysis or interpretation of data; Other

Figure Count:

5

Table Count:

2

Search Terms:

[26] Alzheimer's disease, [120] MRI, Biological subtypes, Disease heterogeneity, Neuropathology

Acknowledgment:**Study Funding:**

This study was funded by the Swedish Foundation for Strategic Research (SSF); the Strategic Research Programme in Neuroscience at Karolinska Institutet (StratNeuro); the Swedish Research Council (VR); the regional agreement on medical training and clinical research (ALF) between Stockholm County Council and Karolinska Institutet; Center for Innovative Medicine (CIMED); the Swedish Alzheimer Foundation; the Swedish Brain Foundation; the Åke Wiberg Foundation; Demensfonden; Stiftelsen Olle Engkvist Byggmästare; Birgitta och Sten Westerberg; Foundation for Geriatric Diseases at Karolinska Institutet; Loo och Hans Ostermans stiftelse för medicinsk forskning; Stiftelsen För Gamla Tjänarinnor; Gun & Bertil Stohnes Stiftelse. MJG is supported by the "Miguel Servet" program [CP19/00031] and a research grant [PI20/00613] of the Instituto de Salud Carlos III-Fondo Europeo de Desarrollo Regional (ISCIII-FEDER). The funding sources did not have any involvement in the study design; collection, analysis, and interpretation of data; writing of the report; and the decision to submit the article for publication. Data collection and sharing for this study was funded by the Alzheimer's Disease Neuroimaging Initiative (ADNI) (National Institutes of Health Grant U01 AG024904) and DOD ADNI (Department of Defense award number W81XWH-12-2-0012). ADNI is funded by the National Institute on Aging, the National Institute of Biomedical Imaging and Bioengineering, and through generous contributions from the following: Alzheimer's Association; Alzheimer's Drug Discovery Foundation; BioClinica, Inc.; Biogen Idec Inc.; Bristol-Myers Squibb Company; Eisai Inc.; Elan Pharmaceuticals, Inc.; Eli Lilly and Company; F. Hoffmann-La Roche Ltd and its affiliated company Genentech, Inc.; GE Healthcare; Innogenetics, N.V.; IXICO Ltd.; Janssen Alzheimer Immunotherapy Research & Development, LLC.; Johnson & Johnson Pharmaceutical Research & Development LLC.; Medpace, Inc.; Merck & Co., Inc.; Meso Scale Diagnostics, LLC.; NeuroRx Research; Novartis Pharmaceuticals Corporation; Pfizer Inc.; Piramal Imaging; Servier; Synarc Inc.; and Takeda Pharmaceutical Company. The Canadian Institutes of Health Research is providing funds to support ADNI clinical sites in Canada. Private sector contributions are facilitated by the Foundation for the National Institutes of Health (www.fnih.org). The grantee organization is the Northern California Institute for Research and Education, and the study is coordinated by the Alzheimer's Disease Cooperative Study at the University of California, San Diego. ADNI data are disseminated by the Laboratory for Neuro Imaging at the University of California, Los Angeles.

Disclosures:

The authors report no disclosures relevant to the manuscript.

Preprint DOI:

<https://doi.org/10.1101/2021.09.06.21263162>

Received Date:

2021-10-22

Accepted Date:

2022-03-04

Handling Editor Statement:

Submitted and externally peer reviewed. The handling editors were Rawan Tarawneh, MD and Brad Worrall, MD, MSc, FAAN.

Abstract

Objectives: To investigate whether antemortem MRI-based atrophy subtypes of Alzheimer's disease (AD) differ in neuropathological features and comorbid non-AD pathologies at postmortem.

Methods: From the ADNI cohort, we included individuals with: antemortem MRI evaluating brain atrophy within 2y before death; antemortem diagnosis of AD dementia/mild cognitive impairment; postmortem-confirmed AD neuropathologic change. Antemortem atrophy subtypes were modeled as continuous phenomena based on a recent conceptual framework: *typicality* (spanning *limbic-predominant AD* to *hippocampal-sparing AD*) and *severity* (spanning *typical AD* to *minimal atrophy AD*). Postmortem neuropathological evaluation included AD hallmarks, amyloid-beta and tau as well as non-AD pathologies, alpha-synuclein and TAR DNA-binding protein-43 (TDP-43). We also investigated the overall concomitance across these pathologies. Partial correlations assessed the associations between antemortem atrophy subtypes and postmortem neuropathological outcomes.

Results: In 31 individuals (26 AD dementia/5 mild cognitive impaired, mean age=80y, 26% females), antemortem typicality was significantly negatively associated with neuropathological features, including amyloid-beta ($\rho=-0.39$ overall), tau ($\rho=-0.38$ regionally), alpha-synuclein ($\rho=-0.39$ regionally), TDP-43 ($\rho=-0.49$ overall), and concomitance of pathologies ($\rho=-0.59$ regionally). Limbic-predominant AD was associated with higher Thal phase, neuritic plaque density, and presence of TDP-43 compared to hippocampal-sparing AD. Regionally, limbic-predominant AD showed higher presence of tau and alpha-synuclein pathologies in medial temporal structures, higher presence of TDP-43

and concomitance of pathologies subcortically/cortically compared to hippocampal-sparing AD. Antemortem severity was significantly negatively associated with concomitance of pathologies ($\rho=-0.43$ regionally), such that typical AD showed higher concomitance of pathologies than minimal atrophy AD.

Discussion: We provide a direct antemortem-to-postmortem validation, highlighting the importance of understanding atrophy-based heterogeneity in AD relative to AD and non-AD pathologies. We suggest that: (a) typicality and severity in atrophy reflect differential aspects of susceptibility of the brain to AD and non-AD pathologies; (b) limbic-predominant AD and typical AD subtypes share similar biological pathways, making them more vulnerable to AD and non-AD pathologies compared to hippocampal-sparing AD, which may follow a different biological pathway. Our findings provide a deeper understanding of associations of atrophy subtypes in AD with different pathologies, enhancing prevailing knowledge of biological heterogeneity in AD and could contribute towards tracking disease progression and designing clinical trials in the future.

Keywords: Alzheimer's disease, neuropathology, postmortem, MRI, antemortem, biological subtypes, Heterogeneity, Amyloid, Tau, TDP-43, Alpha-synuclein, Lewy bodies

Introduction

Alzheimer's disease (AD) is pathologically defined by the hallmarks of amyloid beta (A β) plaques and tau neurofibrillary tangles (NFT). However, pure AD is increasingly recognized as not being the most prevalent form of the disease^{1–3}. Concomitant forms of pathological proteins such as α -synuclein (α -syn) and TAR DNA-binding protein 43 (TDP-43) have been reported in over 40%⁴ and 50%⁵ of the AD cases respectively.

Does this multimorbid view of the brain in AD suggest that atrophy may be downstream to not only the AD hallmark pathologies, but also to the interactions with one or more concomitant pathologies? De Flores et al. examined medial temporal atrophy measured on antemortem magnetic resonance imaging (MRI) in relation to postmortem neuropathology and reported that tau pathology was associated with posterior hippocampal atrophy, whereas TDP-43 pathology was associated with anterior medial temporal atrophy⁶. Medial temporal atrophy, although a common characteristic, is not always observed in AD. Converging evidence suggests that biological heterogeneity in AD may manifest as distinct atrophy subtypes: *typical AD*, *limbic-predominant AD*, *hippocampal-sparing AD*, and *minimal-atrophy AD*⁷, with the last two showing relatively preserved medial temporal gray matter structure. Thus, revising the initial question, we ask: does this multimorbid view of the brain in AD suggest that atrophy *subtypes* may be downstream to not only the AD hallmark pathologies, but also to the interactions with one or more concomitant pathologies? To our knowledge, the answer to this question is yet to be explored.

We currently lack *in vivo* biomarkers to assess pathologies such as α -syn and TDP-43. Therefore, we investigated the relationship between antemortem MRI-based atrophy subtypes and postmortem neuropathological profiles in AD. Our key research questions are (a) whether antemortem atrophy subtypes of AD are related to individual and/or concomitance of AD and non-AD pathologies at postmortem, and (b) whether this subtype-to-pathology relationship varies by brain region. Corresponding to these research questions, we hypothesized that antemortem atrophy subtypes of AD may be differentially associated with different AD and non-AD pathologies assessed postmortem, which may vary by brain region.

Methods

Participants

Participants were selected from the Alzheimer's Disease Neuroimaging Initiative (ADNI) database (PI: M. Weiner; <http://adni.loni.usc.edu/>). Launched in 2003, the goal of the ADNI is to test and use biomarkers, clinical and neuropsychological assessments to track disease progression in AD. We included data from participants who had antemortem MRI and postmortem neuropathological assessments (Version 11, 04/12/2018). **eFigure 1** shows the selection criteria for this study. Our final cohort comprised 31 participants with intermediate or high AD neuropathologic change (ADNC) at postmortem examination (i.e., pathology-confirmed AD dementia; low ADNC is not an adequate explanation for cognitive impairment or dementia)⁹ and availability of an antemortem MRI scan within 2 years prior to death (for a more accurate antemortem approximation of the postmortem/final subtype of an individual and to avoid long antemortem-to-postmortem interval being a potential confound).

Standard Protocol Approvals, Registrations, and Patient Consents

All the ADNI protocols were approved by the institutional review boards of each participating institution. All participants provided written and informed consent in accordance with the Declaration of Helsinki.

Antemortem neuroimaging and cognition

MRI scans were acquired on 1.5T or 3T scanners with T1-weighted sagittal 3D magnetization-prepared rapid gradient echo (MPRAGE) sequences (detailed ADNI imaging protocols: adni.loni.usc.edu/methods/). MRI were processed cross-sectionally using FreeSurfer 6.0.0 (<http://freesurfer.net/>), automated through TheHiveDB system¹⁰. Resulting segmentations were visually screened for quality control. Screened scans were included for subsequent analyses. Automatic region of interest parcellation yielded volumes of 41 cortical and subcortical areas^{11, 12} per hemisphere, serving as a measure of brain atrophy. We used mini mental state examination (MMSE)¹³, clinical dementia rating (CDR), and composite scores for memory (ADNI-MEM)⁴⁸, and executive function (ADNI-EF)⁴⁹ corresponding to the MRI visit as the main outcomes to evaluate the level of cognitive impairment.

Antemortem atrophy subtypes

Following the recently proposed conceptual framework for AD subtypes⁷, we quantified MRI-based atrophy subtypes in terms of two principal dimensions: typicality and severity. Given the limited sample size, we modeled atrophy subtypes on a continuous scale for

greater sensitivity¹⁴ rather than categorizing individuals into subgroups or categorical subtypes. *Typicality* was proxied by the ratio of hippocampal volume to whole cortical volume (ratio henceforth referred to as *H:C*), similar to the index adopted by the original neuropathological subtyping study¹⁵. *Severity* was proxied by the global brain atrophy index, measured by the ratio of whole brain volume to volume of cerebrospinal fluid¹⁶ (ratio henceforth referred to as *BV:CSF*), such that lower values of the index correspond to more atrophy (i.e. higher severity).

Postmortem Neuropathological Assessment

Neuropathological assessments were conducted as part of the ADNI neuropathology core (neuropathologist: Dr. Nigel Cairns, the Knight Alzheimer's Disease Research Center, Washington University School of Medicine, St. Louis, <http://adni.loni.usc.edu/about/#core-container>)¹⁷. Assessments followed the NIA-AA guidelines for the neuropathological assessment of AD⁹ (<https://www.alz.washington.edu/NONMEMBER/NP/npguide10.pdf>).

Antemortem-to-Postmortem Validation Approach

We modeled MRI-based antemortem atrophy subtypes in AD as continuous phenomena¹⁴ of two orthogonal *typicality* and *severity* dimensions, following the recent conceptual framework for AD subtypes⁷. We then examined the relationship of these dimensions to postmortem neuropathological features including AD ($A\beta$, tau), non-AD (α -syn, TDP-43) pathologies and concomitance across them.

To investigate our first research question of whether antemortem atrophy subtypes of AD may be related to neuropathological differences, we examined: (a) established semi-quantitative rating scales for AD-specific neuropathological measures, including Thal phase of regional distribution of A β (diffuse and cored) plaques (A0-A3), Braak stage of NFT distribution (B0-B3), and the Consortium to Establish a Registry for Alzheimer's Disease (CERAD) scores for density of neuritic plaques (C0-C3)⁹; and (b) presence/absence of comorbid non-AD pathologies, including overall α -syn (Lewy body, LB) pathology, assessed across the brainstem, limbic region, neocortex, amygdala and olfactory bulb as per the modified McKeith criteria^{9,18}, and overall TDP-43 pathology assessed as immunoreactive inclusions (comprising any of neuronal cytoplasmic inclusion, NCI, neuronal intraneuronal inclusion, dystrophic neurite or glial cytoplasmic inclusion) across the amygdala, hippocampus, entorhinal cortex/inferior temporal gyrus, and frontal neocortex¹⁹.

To investigate our second research question of whether antemortem atrophy subtypes of AD may be related to postmortem pathologies varying by brain regions, we examined regional pathological outcomes: we analyzed regions most relevant to atrophy subtypes in AD⁷, i.e., structures of the medial temporal lobe including the hippocampus at the level of the lateral geniculate nucleus (cornu Ammonis1 or CA1, dentate gyrus, parahippocampal gyrus), amygdala and entorhinal cortex, and structures of the association cortex including the middle frontal gyrus, superior and middle temporal gyri and inferior parietal lobe (angular gyrus). We focused on specific forms of pathologies binarized for presence/absence: (a) AD-specific neuropathological measures of A β (positive for both

diffuse and cored plaques) and tau (NFT); and (b) non-AD-specific neuropathological measures of α -syn (LB) and TDP-43 (NCI).

To investigate whether antemortem atrophy subtypes of AD may be related to concomitance of pathologies which may also vary regionally, we evaluated the total number of pathologies present per region as an outcome: each pathology was binarized for presence/absence and summed, considering both AD-specific and non-AD-specific pathologies (concomitance ranging from 0 through 4).

Statistical analysis

We analyzed the association between antemortem atrophy subtypes (typicality and severity as continuous independent variables in separate models) and cognition as well as neuropathological outcomes as dependent variables using linear partial correlations, controlled for age at MRI scan, MRI scanner field strength. Further, each model with typicality as independent variable was controlled for severity and vice-versa, to examine if the correlation may be solely explainable by the dimension treated as independent variable. Due to the limited sample size in this rare antemortem-postmortem data set, we report significant results at an uncorrected p -value < 0.05 , akin to previous radiological-pathological association studies^{20,21}. Additionally, we assessed the role of sex (binarized as female or male) and *APOE* status (categorized by all combinations of pairs of the alleles, i.e., 2-4, 3-3, 3-4, 4-4) through mediation analyses⁴⁷.

All statistical analyses and visualizations were conducted using MATLAB R2020b (The MathWorks, Inc., Natick, Massachusetts, USA).

Data Availability

Data used in this study have been made publicly available by the ADNI in the Laboratory of Neuro Imaging database.

Results

Participants

Table 1 shows the demographic and ante-/postmortem characteristics of the cohort. The age at antemortem MRI was 80.0 ± 6.7 y while the age at death was 81.2 ± 6.78 y. The level of cognitive impairment was higher in individuals with AD dementia than those with amnesic mild cognitive impairment (aMCI) in the cohort based on MMSE, CDR, ADNI-MEM, and ADNI-EF. All individuals had markers of cerebrovascular disease postmortem (one or more types of the following: macroscopic vascular brain injury, microinfarcts, microbleeds, microhemorrhages, arteriolosclerosis, white matter rarefaction or other vascular changes).

Antemortem atrophy subtypes

Figure 1A shows the atrophy subtypes in antemortem MRI, characterized by the continuous-scale measures of typicality (H:C) and severity (BV:CSF). We show four examples to illustrate the extremes on each dimension. On the typicality dimension, case RID 1203 represents

hippocampal-sparing AD towards the higher extreme while case RID 1393 represents limbic-predominant AD towards the lower extreme. Similarly, on the severity scale, case RID 1271 represents typical AD towards the lower extreme (higher severity) while case RID 1425 represents minimal-atrophy AD towards the higher extreme (lower severity). The association between typicality and severity was not statistically significant ($r=0.3$, $p=0.09$). Antemortem severity ($r=0.5$, $p=0.01$; controlled for typicality) but not typicality ($r=-0.1$, $p=0.6$; controlled for severity) was significantly associated with MMSE.

Association between antemortem typicality and neuropathological outcomes

Table 2 shows the association between typicality and established neuropathological rating scales of AD and non-AD pathologies. Most individuals showed a high ADNC at postmortem (**Figure 1B**). Typicality was significantly associated with Thal A β phase (96.8% at A3, i.e., Phase 4-5; **Figure 2A**), neuritic plaques (87.1% at C3, i.e., frequent neuritic plaques; **Figure 2C**) and presence of TDP-43 inclusions (**Figure 3B**). These significant associations were negative, i.e., a lower value of H:C (limbic-predominant AD) was associated with higher pathologic burden or presence of pathology.

Figure 4A shows the association between typicality and regional neuropathological measures. Typicality was significantly associated with presence of: (a) tau in the dentate gyrus; (b) α -Syn in the parahippocampal gyrus; (c) TDP-43 in the parahippocampal gyrus, dentate gyrus, entorhinal cortex, amygdala, superior/middle temporal gyri; and (d) concomitance of the AD and non-AD pathologies. These associations were negative, i.e., a

lower value of H:C (limbic-predominant AD) was associated with presence of pathology or higher concomitance of pathologies (**eFigure 2-3**).

Association between antemortem severity and neuropathological outcomes

There were no significant associations between severity and established neuropathological rating scales of AD and non-AD pathologies (**Table 2**).

Neither were there any significant associations between severity and regional neuropathological measures (**Figure 4B**). However, severity was negatively associated with concomitance of AD and non-AD pathologies in the entorhinal cortex. This indicates that a lower value of BV:CSF showed higher concomitance of multiple pathologies (**eFigure 3**).

Antemortem atrophy subtypes and primary and secondary postmortem diagnosis

The primary neuropathological diagnosis was ADNC in all individuals (**Figure 1B**). Several cases had a secondary neuropathological diagnosis (**Figure 1C**), including LB disease (n=16, 51.610%), medial temporal TDP-43 pathology and/or hippocampal sclerosis (n=4, 12.900%), and cerebrovascular pathology (subdural hemorrhage, intracerebral hemorrhage, and/or subcortical arteriosclerotic leukoencephalopathy (n=3, 9.690%). Qualitatively, cases assigned to have TDP-43 in the medial temporal lobe or hippocampal sclerosis inclined towards limbic-predominant AD or typical AD. Cases assigned to have LB pathology tended to be limbic-predominant (dementia with LB pathology), hippocampal-sparing AD (amygdala-predominant LB pathology) or minimal-atrophy AD (both forms). The single isolated cases

with intracerebral hemorrhage, subdural hemorrhage and subcortical arteriosclerotic leukoencephalopathy tended towards minimal-atrophy AD.

The role of sex and APOE status as mediators

Corresponding to each significant association detected, we found that neither sex nor APOE status were likely mediators of the antemortem-postmortem relationship.

Discussion

Our study investigated the relationship between antemortem atrophy subtypes and combinations of different AD and non-AD pathologies assessed postmortem. Heterogeneity in AD is a multifaceted phenomenon involving combinations of protective factors, risk factors and concomitance of non-AD pathologies⁷. The relative contribution of different pathologies to disease heterogeneity has been primarily reported from the postmortem (neuropathological) perspective^{15,22–26} with only one study offering an antemortem (neuroimaging) perspective²⁷, to our knowledge. Our study serves as a direct antemortem-to-postmortem investigation examining the interplay of different pathologies in atrophy subtypes of AD.

From the antemortem perspective, we treated biological heterogeneity in atrophy as continuous phenomena¹⁴, i.e., we examined an MRI-based operationalization of the conceptual framework for AD subtypes in terms of typicality and severity⁷. This approach is complementary to previous studies which conventionally categorize individuals into distinct

subtypes^{28–31}. We observed a non-significant association between typicality and severity, suggesting that disease typicality (proxied by H:C) may not be influenced by disease staging or severity (proxied by BV:CSF), thus serving as orthogonal dimensions of heterogeneity. It is important, however, to note that our initial approach of treating typicality and severity dimensions separately (while controlling for the other dimension) may be rather simplistic and deserves future exploration. This is best exemplified by cases RID 1203 and RID 1452 (**Figure 1A**). Despite having a lower severity (higher BV:CSF), case RID 1203 was described as hippocampal-sparing AD rather than a minimal-atrophy AD. Thus, the combined contribution of typicality and severity must be factored in, i.e., every individual along the typicality dimension must also be interpreted in conjunction with the corresponding severity level and vice-versa.

Our key finding was that antemortem typicality, but not severity, was associated with different pathologies observed postmortem including A β , tau, α -syn, and TDP-43. One reasoning for the lack of association between antemortem severity and postmortem pathologies could be that most individuals were at advanced disease stages (high ADNC), contributing to a low variability in postmortem disease severity. Below we discuss the role of individual pathologies in relation to antemortem heterogeneity in atrophy.

Amyloid pathology: We found an association between typicality and Thal A β stages, suggesting lower A β in hippocampal-sparing AD *atrophy* subtype, which is consistent with a recent meta-analysis evaluating the proportion of A β positivity in this subtype⁷. This result may be expected given that A β hallmark pathology in AD is rather diffuse, which may be

indirectly associated with some degree of downstream atrophy³². However, we did not find a significant association of typicality with regional ratings of A β density, perhaps because A β accumulation is usually widespread and homogeneous, with little regional specificity. To some degree, this lack of regional associations likely reflects the lack of topographical correspondence between A β and atrophy, as evidence suggests a closer relationship between atrophy and tau than atrophy and A β ^{33–35}.

Tau pathology: We did not observe an association between typicality or severity and Braak NFT stages even though the AD dementia cases (N=26 at Braak stage V or VI) were at relatively more advanced stages than the aMCI (N=5 at Braak stage III or V). This lack of association is most likely due to little variability in this measure, as all but two cases (Braak stage III, both aMCI) were at Braak stages V or VI. When assessing NFT load regionally, however, limbic-predominant AD *atrophy* subtype was associated with presence of tau pathology in the hippocampus. This is not surprising since tau pathology is a hallmark of AD affecting the hippocampus, particularly the dentate gyrus, which is known to contain the largest density of synapses³⁶. Thus, presence of tau pathology may eventually be reflected in significant atrophy in the region, which is a key characteristic of the limbic-predominant AD *atrophy* subtype. Conversely, the hippocampal-sparing AD *atrophy* subtype was associated with absence of tau pathology in the dentate gyrus of the hippocampus. Supporting evidence for the association between atrophy and tau pathology in this subtype is not straightforward, owing to factors including the interval between assessments of these biomarkers¹⁴, regional non-specificity of atrophy and disagreement of subtyping methods based on these biomarkers⁸. Altogether, our study is useful in providing a direct link

between antemortem atrophy and postmortem tau pathology, suggesting that hippocampal atrophy relative to neocortical atrophy can track postmortem NFT subtypes¹⁵.

α -syn pathology: When assessing α -syn LB pathology regionally, we observed that limbic-predominant AD *atrophy* subtype may be more prone to presence of this pathology. We also found that the parahippocampal gyrus was significantly associated with presence of overall α -syn pathology. These findings corroborate previous postmortem neuropathological studies showing increased α -syn pathology in typical AD and limbic-predominant AD *tau* subtypes^{15,22}. However, other postmortem neuropathological studies have reported increased α -syn pathology in the hippocampal-sparing AD *tau* subtype^{23,24,27}. Moreover, a recent antemortem MRI study in dementia with LB observed predominance of hippocampal-sparing *atrophy* subtype³⁷. It must, however, be noted that most of the postmortem studies reporting presence of α -syn pathology to date have characterized tau subtypes, which are not necessarily interchangeable with atrophy subtypes in AD^{8,14}. Therefore, future *in vivo* investigations are warranted to confirm the role of α -syn pathology in AD heterogeneity. Further, α -syn LB (neocortical) pathology may potentially interact with tau (Braak stage V-VI) pathology and advanced age in our cohort, explaining atrophy in the limbic-predominant AD *atrophy* subtype, given that limbic atrophy is not observable in the absence of these factors³⁸.

TDP-43 pathology: Our most robust findings included the association of limbic-predominant AD *atrophy* subtype with presence of TDP-43 pathology. Limbic-predominant AD *tau* subtype has been described to be more prone to exhibiting TDP-43 in previous postmortem

studies^{15,22,24}. It is thus plausible for the limbic-predominant AD *atrophy* subtype to follow suit, given the topographical similarity between tau and atrophy patterns in limbic-predominant AD¹⁴. Congruent with the report from the recent meta-analysis⁷, our study provides an antemortem-to-postmortem validation and evidence supporting the association of limbic-predominant AD *atrophy* subtype with TDP-43. We observed a gradually increasing number of brain regions being affected by TDP-43 as one moves along the typicality dimension towards limbic-predominant AD. Regional examination revealed the strongest association between typicality and presence of TDP-43 in the amygdala, an initial affected site by this pathology²⁶, as well as in other medial temporal lobe structures (hippocampus, entorhinal cortex), shown to be affected by a recent antemortem study⁶. As a main contributor of pathology affecting the hippocampus, TDP-43-associated hippocampal atrophy may be detectable at least 10 years prior to death³⁹. Thus, the limbic-predominant AD *atrophy* subtype is most likely to exhibit Limbic-predominant age-related TDP-43 encephalopathy neuropathological changes (LATE-NC)⁴⁰. In the absence of *in vivo* biomarkers assessing TDP-43, antemortem atrophy-based typicality (H:C) as a consistent correlate of postmortem TDP-43 in our study indicates the potential of this index as an antemortem proxy for this pathology.

Another main finding of our study was that both typicality and severity were regionally associated with concomitance of pathologies. This relationship was such that limbic-predominant AD and typical AD subtypes were associated with higher concomitance while hippocampal-sparing AD and minimal-atrophy AD subtypes were associated with lower concomitance. There also appears to be a region-specific effect, whereby some regions may

accumulate a greater number of pathologies while other regions may be spared. For example, limbic-predominant AD was associated with higher concomitance of different pathologies, particularly in the medial and superior temporal structures and typical AD was associated with higher pathological concomitance in the entorhinal cortex. Interestingly, hippocampal structures including the dentate gyrus and CA1 demonstrated a generally lower concomitance than other regions. The divergent reports mentioned previously on α -syn pathology being associated with limbic-predominant and typical atrophy subtypes may be due to the higher susceptibility of the subtypes to multiple or mixed pathologies.

Finally, although qualitative, individual-level secondary postmortem diagnoses aided in providing greater confidence to our quantitative findings. Two cases with lower H:C index (towards limbic-predominant AD) were diagnosed to have TDP-43 in the medial temporal region, consistent with our main quantitative findings. Two additional cases with lower H:C index were diagnosed to have hippocampal sclerosis, which is known to correlate well with TDP-43 pathology^{15,22}. Five out of six cases with relatively higher H:C index (towards hippocampal-sparing AD) were assigned to have amygdala-predominant LB pathology, a distinct pathological entity⁴. Whether/how the presence of LB pathology in the amygdala plays a role in the disposition of hippocampal-sparing AD atrophy subtype to the pathology remains to be seen. Three cases with relatively higher H:C (towards hippocampal-sparing AD) and higher BV:CSF (towards minimal-atrophy AD) indices were diagnosed with cerebrovascular pathologies. Although lack of variability in the measure of cerebrovascular disease did not allow us to account for it in our quantitative analyses, these qualitative

observations align with recent evidence, showing that cerebrovascular disease may particularly affect hippocampal-sparing AD⁴¹ and minimal atrophy AD subtypes^{41,42}.

Considering our current findings, we propose two hypotheses for future work as larger antemortem-postmortem datasets become available (**Figure 5**): (a) biological heterogeneity, characterized by the orthogonal dimensions of typicality and severity, capture different aspects of vulnerability of the brain to AD and non-AD pathologies. While typicality may be relatively more sensitive to individual pathologies varying regionally, severity may predominantly reflect a cumulative contribution of several pathologies, measured as concomitance; (b) limbic-predominant AD and typical AD subtypes may follow a unique biological pathway which tends to be affected by greater accumulation, interaction and concomitance of various pathologies, distinct from the pathway followed by hippocampal-sparing AD subtype which may be less affected. It is unclear which pathway the minimal atrophy AD subtype may follow: at antemortem, individuals tending towards minimal atrophy AD were at early disease stages (i.e., amnesic mild cognitive impairment) and could have eventually progressed into one of the other three subtypes, thus possibly following either of the two hypothesized pathways; at postmortem, however, many of these individuals showed high ADNC despite having minimal atrophy, suggesting that minimal atrophy AD may share the pathway common to the hippocampal-sparing AD subtype of being less affected by concomitance of various pathologies. While our current and recent works^{43,44} provide initial support, these hypotheses need to be tested by future studies to understand their potential validity across different modalities (heterogeneity assessed by

measures other than atrophy), pathologies (e.g., vascular burden) and disease stages (including pre-dementia cases).

Our study has some limitations. Firstly, the sample size of our cohort was limited, which may reduce the power to detect significant associations and generalize findings. However, our sample size was comparable to prior studies combining antemortem and postmortem data^{45,46}. Despite the size, we observed representation of four subtypes and we chose methodologies was proportionate to this limited sample size by modeling heterogeneity as the continuous measures (typicality, severity), and analyzing heterogeneity with partial correlation models to maximize statistical power. Secondly, postmortem pathologies were only available as semi-quantitative scores (i.e., gross burden of pathology), which we further binarized for presence/absence of pathologies for sufficient statistical power. These scales may not be as sensitive as quantitative scores obtained from digital histology techniques (e.g., specific counts, density, or percentage of pathology per region). Thirdly, most of the individuals showed a high ADNC (low variability in postmortem severity), which may have influenced the finding that the associations of antemortem MRI typicality with postmortem pathologies were stronger than those of MRI severity. Future investigations should include a broader range of pathological severity to fully explore associations for the severity dimension. Finally, all data were sourced from the ADNI, known to have relatively strict inclusion criteria. Therefore, our current findings would need to be further validated by future studies using less restrictive and more heterogeneous cohorts.

In conclusion, we examined the relationship between antemortem MRI-based atrophy subtypes (modeled as continuous phenomena) and postmortem neuropathology in AD. In our cohort, antemortem typicality shared a stronger overall and region-specific association with different postmortem pathologies including A β , tau, α -synuclein, and TDP-43, compared to antemortem severity. This suggests that the novel operationalization of biological heterogeneity in AD including typicality as a continuum is a promising proxy for presence and regional distribution of pathologies, irrespective of disease staging (severity). Thus, factoring in contributions of core AD and comorbid non-AD pathologies towards biological heterogeneity in unspecific markers of neurodegeneration may subsequently serve as an avenue for precision medicine and future multi-factorial therapies.

WNL-2022-200625_sup --- <http://links.lww.com/WNL/C4>

WNL-2022-200625_coinvestigator_appendix --- <http://links.lww.com/WNL/C7>

References

1. Barker WW, Luis CA, Kashuba A, et al. Relative frequencies of Alzheimer disease, Lewy body, vascular and frontotemporal dementia, and hippocampal sclerosis in the State of Florida Brain Bank. *Alzheimer Dis Assoc Disord*. LWW; 2002;16:203–212.
2. Rahimi J, Kovacs GG. Prevalence of mixed pathologies in the aging brain. *Alzheimer's Res Ther*. Springer; 2014;6:1–11.
3. Spires-Jones TL, Attems J, Thal DR. Interactions of pathological proteins in neurodegenerative diseases. *Acta Neuropathol*. Springer; 2017;134:187–205.
4. Uchikado H, Lin W-L, DeLucia MW, Dickson DW. Alzheimer disease with amygdala Lewy bodies: a distinct form of α -synucleinopathy. *J Neuropathol Exp Neurol*. American Association of Neuropathologists; 2006;65:685–697.
5. Josephs KA, Murray ME, Whitwell JL, et al. Updated TDP-43 in Alzheimer's disease staging scheme. *Acta Neuropathol*. Springer; 2016;131:571–585.
6. de Flores R, Wisse LEM, Das SR, et al. Contribution of mixed pathology to medial temporal lobe atrophy in Alzheimer's disease. *Alzheimer's Dement*. Wiley Online Library; 2020;16:843–852.
7. Ferreira D, Nordberg A, Westman E. Biological subtypes of Alzheimer disease: A systematic review and meta-analysis. *Neurology*. AAN Enterprises; 2020;94:436–448.
8. Mohanty R, Mårtensson G, Poulakis K, et al. Comparison of subtyping methods for

neuroimaging studies in Alzheimer's disease: a call for harmonization. *Brain Commun.* 2020;2:fcaa192.

9. Montine TJ, Phelps CH, Beach TG, et al. National Institute on Aging–Alzheimer's Association guidelines for the neuropathologic assessment of Alzheimer's disease: a practical approach. *Acta Neuropathol.* Springer; 2012;123:1–11.
10. Muehlboeck J, Westman E, Simmons A. TheHiveDB image data management and analysis framework. *Front Neuroinform.* Frontiers; 2014;7:49.
11. Desikan RS, Ségonne F, Fischl B, et al. An automated labeling system for subdividing the human cerebral cortex on MRI scans into gyral based regions of interest. *Neuroimage.* Elsevier; 2006;31:968–980.
12. Fischl B, Salat DH, Busa E, et al. Whole brain segmentation: automated labeling of neuroanatomical structures in the human brain. *Neuron.* Elsevier; 2002;33:341–355.
13. Folstein MF, Folstein SE, McHugh PR. "Mini-mental state": a practical method for grading the cognitive state of patients for the clinician. *J Psychiatr Res.* Pergamon; 1975;12:189–198.
14. Mohanty R, Ferreira D, Nordberg A, Westman E. Associations between different tau-PET patterns and longitudinal atrophy in the Alzheimer's disease continuum. *medRxiv.* Cold Spring Harbor Laboratory Press; Epub 2021.
15. Murray ME, Graff-Radford NR, Ross OA, Petersen RC, Duara R, Dickson DW. Neuropathologically defined subtypes of Alzheimer's disease with distinct clinical characteristics: a retrospective study. *Lancet Neurol.* Elsevier; 2011;10:785–796.
16. Orellana C, Ferreira D, Muehlboeck J-S, et al. Measuring global brain atrophy with the

brain volume/cerebrospinal fluid index: normative values, cut-offs and clinical associations. *Neurodegener Dis*. Karger Publishers; 2016;16:77–86.

17. Franklin EE, Perrin RJ, Vincent B, et al. Brain collection, standardized neuropathologic assessment, and comorbidity in Alzheimer's Disease Neuroimaging Initiative 2 participants. *Alzheimer's Dement*. Elsevier; 2015;11:815–822.
18. McKeith IG, Dickson DW, Lowe J, et al. Diagnosis and management of dementia with Lewy bodies: third report of the DLB Consortium. *Neurology*. AAN Enterprises; 2005;65:1863–1872.
19. Katsumata Y, Fardo DW, Kukull WA, Nelson PT. Dichotomous scoring of TDP-43 proteinopathy from specific brain regions in 27 academic research centers: associations with Alzheimer's disease and cerebrovascular disease pathologies. *Acta Neuropathol Commun*. BioMed Central; 2018;6:1–11.
20. Wisse LEM, de Flores R, Xie L, et al. Pathological drivers of neurodegeneration in suspected non-Alzheimer's disease pathophysiology. *Alzheimers Res Ther*. Springer; 2021;13:1–11.
21. Spina S, La Joie R, Petersen C, et al. Comorbid neuropathological diagnoses in early versus late-onset Alzheimer's disease. *Brain*. Epub 2021.
22. Janocko NJ, Brodersen KA, Soto-Ortolaza AI, et al. Neuropathologically defined subtypes of Alzheimer's disease differ significantly from neurofibrillary tangle-predominant dementia. *Acta Neuropathol*. Springer; 2012;124:681–692.
23. Jellinger KA. Neuropathological subtypes of Alzheimer's disease. *Acta Neuropathol*. Springer Nature BV; 2012;123:153.

24. Josephs KA, Whitwell JL, Tosakulwong N, et al. TAR DNA-binding protein 43 and pathological subtype of Alzheimer's disease impact clinical features. *Ann Neurol*. Wiley Online Library; 2015;78:697–709.
25. Murray ME, Cannon A, Graff-Radford NR, et al. Differential clinicopathologic and genetic features of late-onset amnesic dementias. *Acta Neuropathol*. Springer; 2014;128:411–421.
26. Hu WT, Josephs KA, Knopman DS, et al. Temporal lobar predominance of TDP-43 neuronal cytoplasmic inclusions in Alzheimer disease. *Acta Neuropathol*. Springer; 2008;116:215.
27. Whitwell JL, Dickson DW, Murray ME, et al. Neuroimaging correlates of pathologically defined subtypes of Alzheimer's disease: a case-control study. *Lancet Neurol*. Elsevier; 2012;11:868–877.
28. Ferreira D, Verhagen C, Hernández-Cabrera JA, et al. Distinct subtypes of Alzheimer's disease based on patterns of brain atrophy: longitudinal trajectories and clinical applications. *Sci Rep*. Nature Publishing Group; 2017;7:46263.
29. Poulakis K, Pereira JB, Mecocci P, et al. Heterogeneous patterns of brain atrophy in Alzheimer's disease. *Neurobiol Aging*. Elsevier; 2018;65:98–108.
30. Byun MS, Kim SE, Park J, et al. Heterogeneity of regional brain atrophy patterns associated with distinct progression rates in Alzheimer's disease. *PLoS One*. Public Library of Science; 2015;10:e0142756.
31. Risacher SL, Anderson WH, Charil A, et al. Alzheimer disease brain atrophy subtypes are associated with cognition and rate of decline. *Neurology*. AAN Enterprises;

2017;89:2176–2186.

32. Iaccarino L, Tammewar G, Ayakta N, et al. Local and distant relationships between amyloid, tau and neurodegeneration in Alzheimer's Disease. *NeuroImage Clin.* Elsevier; 2018;17:452–464.
33. Nelson PT, Alafuzoff I, Bigio EH, et al. Correlation of Alzheimer disease neuropathologic changes with cognitive status: a review of the literature. *J Neuropathol Exp Neurol.* Oxford University Press; 2012;71:362–381.
34. Gordon BA, McCullough A, Mishra S, et al. Cross-sectional and longitudinal atrophy is preferentially associated with tau rather than amyloid β positron emission tomography pathology. *Alzheimer's Dement Diagnosis, Assess Dis Monit.* Elsevier; 2018;10:245–252.
35. Ossenkoppele R, Smith R, Mattsson-Carlsson N, et al. Accuracy of Tau Positron Emission Tomography as a Prognostic Marker in Preclinical and Prodromal Alzheimer Disease: A Head-to-Head Comparison Against Amyloid Positron Emission Tomography and Magnetic Resonance Imaging. *JAMA Neurol.* Epub 2021.
36. Lace G, Savva GM, Forster G, et al. Hippocampal tau pathology is related to neuroanatomical connections: an ageing population-based study. *Brain.* Oxford University Press; 2009;132:1324–1334.
37. Oppedal K, Ferreira D, Cavallin L, et al. A signature pattern of cortical atrophy in dementia with Lewy bodies: a study on 333 patients from the European DLB consortium. *Alzheimer's Dement.* Elsevier; 2019;15:400–409.
38. Ferman TJ, Aoki N, Boeve BF, et al. Subtypes of dementia with Lewy bodies are

associated with α -synuclein and tau distribution. *Neurology*. AAN Enterprises; 2020;95:e155–e165.

39. Josephs KA, Dickson DW, Tosakulwong N, et al. Rates of hippocampal atrophy and presence of post-mortem TDP-43 in patients with Alzheimer's disease: a longitudinal retrospective study. *Lancet Neurol*. Elsevier; 2017;16:917–924.
40. Nelson PT, Dickson DW, Trojanowski JQ, et al. Limbic-predominant age-related TDP-43 encephalopathy (LATE): consensus working group report. *Brain*. Oxford University Press; 2019;142:1503–1527.
41. Ferreira D, Shams S, Cavallin L, et al. The contribution of small vessel disease to subtypes of Alzheimer's disease: a study on cerebrospinal fluid and imaging biomarkers. *Neurobiol Aging*. Elsevier; 2018;70:18–29.
42. Ferreira D, Wahlund L-O, Westman E. The heterogeneity within Alzheimer's disease. *Aging (Albany NY)*. Impact Journals, LLC; 2018;10:3058.
43. Poulakis K, Pereira JB, Muehlboeck J, et al. Stage vs. Subtype Hypothesis in Alzheimer's Disease: A Multi-Cohort and Longitudinal Bayesian Clustering Study.
44. Ferreira, Daniel; Mohanty, Rosaleena; Murray, Melissa; Nordberg, Agneta; Kantarci, Kejal; Westman E. Does a truly hippocampal sparing subtype of Alzheimer's disease really exist? 2021 Alzheimer's Assoc Int Conf. 2021.
45. Teipel SJ, Fritz H-C, Grothe MJ, Initiative ADN. Neuropathologic features associated with basal forebrain atrophy in Alzheimer disease. *Neurology*. AAN Enterprises; 2020;95:e1301–e1311.
46. Grothe MJ, Moscoso A, Ashton NJ, et al. Associations of Fully Automated CSF and

Novel Plasma Biomarkers With Alzheimer Disease Neuropathology at Autopsy.

Neurology. AAN Enterprises; Epub 2021.

47. Baron RM, Kenny DA. The moderator–mediator variable distinction in social psychological research: Conceptual, strategic, and statistical considerations. *J Pers Soc Psychol*. American Psychological Association; 1986;51:1173.
48. Crane PK, Carle A, Gibbons LE, et al. Development and assessment of a composite score for memory in the Alzheimer’s Disease Neuroimaging Initiative (ADNI). *Brain Imaging Behav*. Springer; 2012;6:502–516.
49. Gibbons LE, Carle AC, Mackin RS, et al. A composite score for executive functioning, validated in Alzheimer’s Disease Neuroimaging Initiative (ADNI) participants with baseline mild cognitive impairment. *Brain Imaging Behav*. Springer; 2012;6:517–527.

Table 1. Characteristics of the selected cohort

N		31
Age at antemortem MRI (y)		80.032 ± 6.745
MRI field strength (% 3 Tesla)		41.940
Age at death (y)		81.226 ± 6.781
Antemortem MRI to postmortem interval (y)		1.193 ± 0.601
Diagnosis at antemortem MRI		26 AD Dementia, 5 aMCI
Sex (% female)		25.810
Education (y)		16.129 ± 2.247
APOE ε4 (% carriers)		80.650
MMSE at antemortem MRI	Overall	18.161 ± 6.738
	AD Dementia	16.461 ± 5.846
	aMCI	27 ± 3.240
CDR at antemortem MRI	Overall	1.339 ± 0.723
	AD Dementia	1.500 ± 0.678
	aMCI	0.500 ± 0
ADNI-MEM at antemortem MRI	Overall	-1.268 ± 1.001
	AD Dementia	-1.515 ± 0.814
	aMCI	0.012 ± 0.968
ADNI-EF at antemortem MRI	Overall	-1.455 ± 1.312
	AD Dementia	-1.779 ± 1.147
	aMCI	0.165 ± 0.802
Presence of markers of cerebrovascular disease postmortem (%)		100

Abbreviations: MRI=magnetic resonance imaging; AD=Alzheimer's disease; aMCI=amnesic mild cognitive impairment; APOE=apolipoprotein; MMSE=mini mental state examination; CDR=clinical dementia rating; ADNI-MEM=composite cognitive score for memory; ADNI-EF=composite cognitive score for executive function.

Table 2. Association of antemortem atrophy subtype dimensions with AD neuropathological rating scales and presence of comorbid non-AD pathologies

Postmortem pathology	Antemortem Typicality rho (<i>p</i>)	Antemortem Severity rho (<i>p</i>)
Thal A β phase	-0.39 (0.035)	0.18 (0.37)
Braak Tau stage	-0.19 (0.32)	-0.18 (0.35)
Neuritic plaque	-0.40 (0.034)	0.18 (0.61)
α -syn	-0.03 (0.86)	-0.21 (0.29)
TDP-43 inclusions	-0.49 (0.011)	-0.16 (0.46)

Note: Overall α -syn was evaluated across brainstem-predominant, limbic/transitional, neocortical/diffuse and amygdala-predominant stages) and overall TDP-43 was evaluated across amygdala, hippocampus, entorhinal/inferior temporal cortex and neocortex. α -syn and TDP-43 pathologies were binarized to evaluate presence or absence; Associations between typicality or severity and individual pathologies were evaluated using partial correlation, adjusted for field strength, age at scan, and the other dimension of subtypes (severity or typicality); rho=linear partial correlation coefficient; $p < 0.05$ are shown in **bold**.

Abbreviation: TDP-43=TAR DNA-binding protein 43.

Figure Legends

Figure 1. Distribution of **(A)** antemortem MRI-based heterogeneity and **(B-C)** postmortem neuropathology superposed on MRI-based heterogeneity

Note: **(A)** antemortem atrophy subtypes modeled as continuous phenomena by the dimensions of typicality and severity. Four individual cases are highlighted showing the extremes on each dimension; **(B)** postmortem AD neuropathologic change; **(C)** postmortem secondary diagnosis assigned per individual. All plots show antemortem MRI-based typicality on the horizontal scale, proxied by the index $= \left(\frac{\text{hippocampal volume}}{\text{cortical volume}} \right)$; All plots show antemortem MRI-based severity on the vertical scale, proxied by the global brain atrophy index $= \left(\frac{\text{total brain volume}}{\text{cerebrospinal fluid volume}} \right)$, whereby higher values correspond to lower severity.

Abbreviations: AD=Alzheimer's disease; aMCI=amnesic mild cognitive impairment; MRI=magnetic resonance imaging; TAD=typical AD; HS=hippocampal-sparing AD; MA=minimal-atrophy AD; LP=limbic-predominant AD; RID=Assigned individual ID in the AD Neuroimaging Initiative dataset; ADNC=AD neuropathological change; ALB=amygdala Lewy bodies; DLB=dementia with Lewy bodies; HS=hippocampal sclerosis; ICH=intracerebral hemorrhage; SAL=subcortical arteriosclerotic leukoencephalopathy; SDH=subdural hemorrhage; TDP-MTL=TAR DNA-binding protein in the medial temporal lobe.

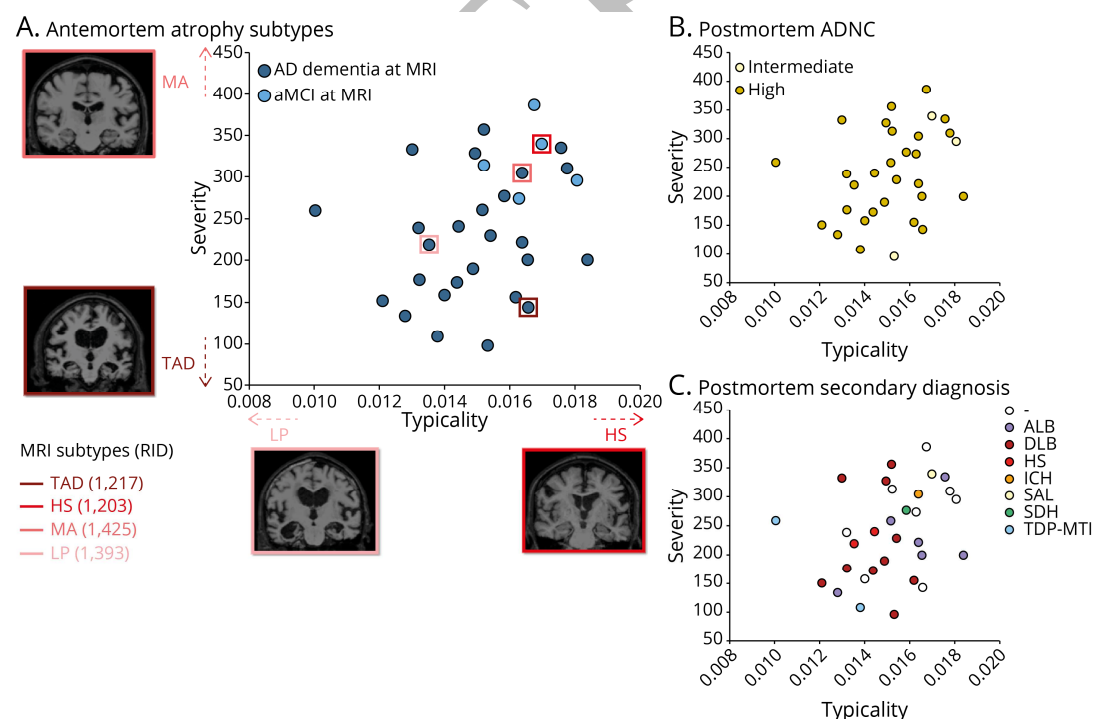


Figure 2. Distribution of postmortem AD neuropathologies superposed on MRI-based heterogeneity

Note: Postmortem AD pathologies used to assess ADNC, encompassing the “ABC” scores of **(A)** Thal phase for A β , **(B)** Braak stage for tau, and **(C)** Consortium to Establish a Registry for AD neuritic plaques. All plots show antemortem MRI-based typicality on the horizontal scale, proxied by the index= $\left(\frac{\text{hippocampal volume}}{\text{cortical volume}}\right)$; All plots show antemortem MRI-based severity on the vertical scale, proxied by the global brain atrophy index= $\left(\frac{\text{total brain volume}}{\text{cerebrospinal fluid volume}}\right)$, whereby higher values correspond to lower severity.

Abbreviations: AD=Alzheimer’s disease; MRI=magnetic resonance imaging; TAD=typical AD; HS=hippocampal-sparing AD; MA=minimal-atrophy AD; LP=limbic-predominant AD; ADNC=AD neuropathological change.

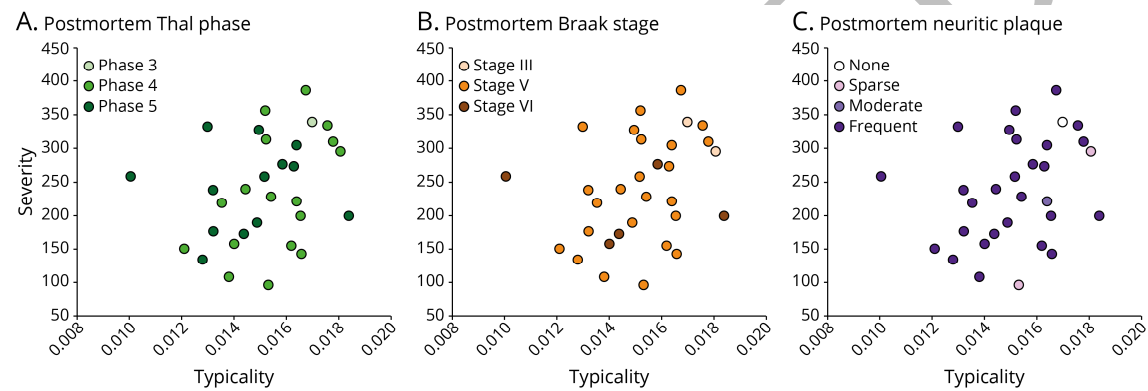


Figure 3. Distribution of postmortem non-AD neuropathologies superposed on MRI-based heterogeneity

Note: Postmortem non-AD pathologies including **(A)** α -synuclein Lewy bodies, and **(B)** TDP-43. All plots show antemortem MRI-based typicality on the horizontal scale, proxied by the index= $\left(\frac{\text{hippocampal volume}}{\text{cortical volume}}\right)$; All plots show antemortem MRI-based severity on the vertical scale, proxied by the global brain atrophy index= $\left(\frac{\text{total brain volume}}{\text{cerebrospinal fluid volume}}\right)$, whereby higher values correspond to lower severity.

Abbreviations: AD=Alzheimer's disease; MRI=magnetic resonance imaging; TAD=typical AD; HS=hippocampal-sparing AD; MA=minimal-atrophy AD; LP=limbic-predominant AD; TDP-43=TAR DNA-binding protein 43; A+E=TDP-43 immunoreactive inclusions are present in the amygdala and entorhinal/inferior temporal cortex; A+H+E=TDP-43 immunoreactive inclusions are present in the amygdala, hippocampus and entorhinal/inferior temporal cortex; A+H+E+N=TDP-43 immunoreactive inclusions are present in the amygdala, hippocampus, entorhinal/inferior temporal cortex and neocortex; ALB=amygdala Lewy bodies; DLB=dementia with Lewy bodies.

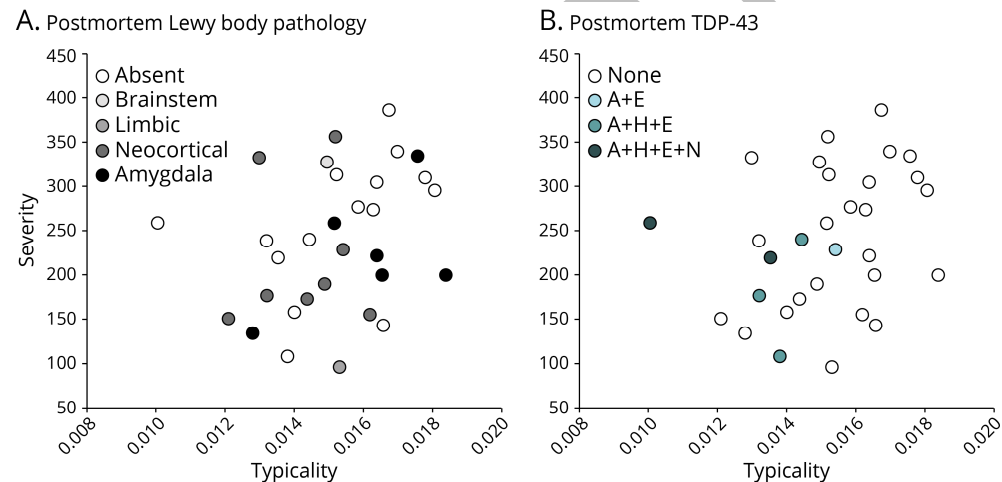


Figure 4. Association between antemortem MRI-based (A) typicality and (B) severity and regional neuropathological features

Note: Associations between each of typicality or severity and presence of regional pathologies were evaluated using linear partial correlation, adjusted for field strength, age at scan, and the other dimension (severity or typicality); Linear partial correlation coefficient (rho) and significant *p*-values are indicated.

Abbreviations: MRI=magnetic resonance imaging; PHG=hippocampus at the level of lateral geniculate nucleus including parahippocampal gyrus; DG=hippocampus at the level of lateral geniculate nucleus including dentate gyrus; CA1=hippocampus at the level of lateral geniculate nucleus including cornu ammonis1 subfield; ERC=entorhinal cortex; AMYG=amygdala; IPL=inferior parietal lobe (angular gyrus); STG=superior and middle temporal gyri; MFG=middle frontal gyrus; A β =beta-amyloid (diffuse and cored plaques); Tau=phosphorylated tau assessing neurofibrillary tangles; α -syn=alpha-synuclein Lewy body pathology; TDP-43=phosphorylated TAR DNA-binding protein 43 neuronal cytoplasmic inclusion.

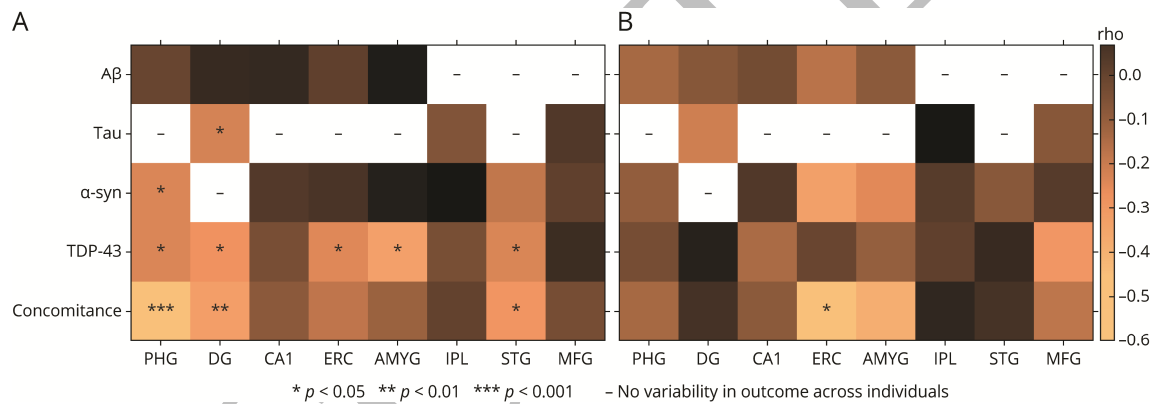
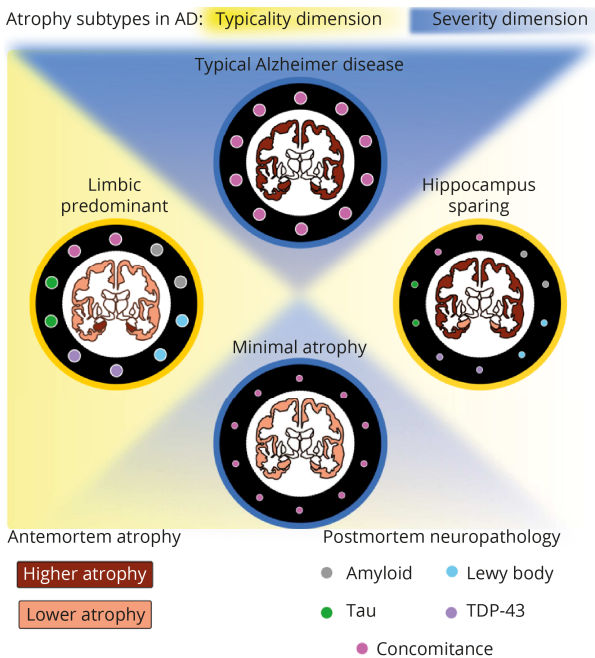


Figure 5. Susceptibility of antemortem MRI-based heterogeneity to AD and non-AD neuropathologies

Associations of antemortem typicality and severity with postmortem neuropathological features may generate the following hypotheses: (a) the orthogonal dimensions of biological heterogeneity, typicality and severity, may offer complementary information regarding the vulnerability of the brain to AD (amyloid, tau) and non-AD (α -syn, TDP-43) pathologies; (b) limbic-predominant AD along the typicality dimension and typical AD along the severity dimension may share similar underlying biological pathway(s), which make them more susceptible to pathologies whereas hippocampal-sparing AD along the typicality dimension and minimal AD long the severity dimension may share similar pathway(s), making them less susceptible.



Neurology®

Neuropathologic Features of Antemortem Atrophy-Based Subtypes of Alzheimer Disease

Rosaleena Mohanty, Daniel Ferreira, Simon Frerich, et al.

Neurology published online May 24, 2022

DOI 10.1212/WNL.0000000000200573

This information is current as of May 24, 2022

Updated Information & Services	including high resolution figures, can be found at: http://n.neurology.org/content/early/2022/05/24/WNL.0000000000200573.full
Subspecialty Collections	This article, along with others on similar topics, appears in the following collection(s): Alzheimer's disease http://n.neurology.org/cgi/collection/alzheimers_disease MRI http://n.neurology.org/cgi/collection/mri
Permissions & Licensing	Information about reproducing this article in parts (figures, tables) or in its entirety can be found online at: http://www.neurology.org/about/about_the_journal#permissions
Reprints	Information about ordering reprints can be found online: http://n.neurology.org/subscribers/advertise

Neurology® is the official journal of the American Academy of Neurology. Published continuously since 1951, it is now a weekly with 48 issues per year. Copyright Copyright © 2022 The Author(s). Published by Wolters Kluwer Health, Inc. on behalf of the American Academy of Neurology.. All rights reserved. Print ISSN: 0028-3878. Online ISSN: 1526-632X.

